J. theor. Biol. (1999) **201,** 251–270
Article No. jtbi.1999.1028, available online at http://www.idealibrary.com on IDEAL®

The Hydraulic System of Trees: Theoretical Framework and Numerical Simulation

THOMAS FRÜH AND WINFRIED KURTH*

Institute of Forest Biometry and Informatics, University of Göttingen, Büsgenweg 4, *D*-37077 *Göttingen, Germany*

(*Received on* 15 *May* 1998, *Accepted in revised form on* 30 *September* 1999)

Empirical studies pose the problem of the physiological integration of the tree organism, which is also important on the scale of ecosystems. Recently, spatially distributed models emerged, which approach this problem by reflecting the close linkage between physiological processes and the structures of trees and tree stands. In the case of water flow, the tree organism can be regarded as hydraulic system and the branched tree architecture as hydraulic network. Previous models of the hydraulic system either did not take into account the network structure, or they had shortcomings regarding the translation of the underlying physiological assumptions by the discrete computation method. We have developed a theoretical framework which takes the form of a numerical simulation model of tree water flow. A discrete initial boundary value problem (IBVP) combines the phenomena of Darcy flow, water storage and conductivity losses in the hydraulic network. The software HYDRA computes the solution of the IBVP. The theoretical derivation and model tests corroborate the consistent translation of the physiological assumptions by the computational method. Simulation studies enabled us to formulate hypotheses on the following points: (1) differences in the hydraulic segmentation between *Picea abies* and *Thuja occidentalis*, (2) responses of the hydraulic system to rapid transpiration changes and to a scenario of drought stress, and (3) how these responses depend on architectural quantities of the trees. The simulation studies demonstrated our possibilities of deriving theoretically well-founded hypotheses about the functioning of the hydraulic system and its relation to system structure. The numerical simulation model is designed as a tool for structure–function studies, which is able to treat tree architecture as independent variable. The model supports the integration of data on tree level, and it can be used for computer experiments which quantify the dynamics of the hydraulic system according to the concepts of system theory.

© 1999 Academic Press

Introduction

Empirical studies give evidence of a close linkage between hydraulic function and the branched structures of trees which are acyclic networks (Swamy & Thulasiraman, 1981) of water flow paths. Within these networks, spatial patterns of hydraulic conductivity are found that correlate with branching parameters (Zimmermann, 1978; Tyree *et al.*, 1983; Ewers & Zimmermann, 1984).

A high atmospherical water demand acts upon the hydraulic system as a stress factor. It can cause low water potentials in the xylem in two ways: by water deficits or by high internal flow rates. These types of stress are termed static and

* Author to whom correspondence should be addressed.
E-mail: wkurth@ufobi4.uni-forst.gwdg.de

0022–5193/99/240251 + 20 $30.00/0
© 1999 Academic Press

dynamic drought stress, though the latter typically occurs near water saturation of the soil (Tyree & Ewers, 1991). Declining xylem water potential leads to a progressive loss of conductivity (Edwards & Jarvis, 1982; Sperry & Tyree, 1990; Sellin, 1991; Cochard, 1992; Pockman *et al.*, 1995; Sperry & Ikeda, 1997). The hydraulic vulnerability depends on species and is associated with the water relations of the species habitat (Tyree & Ewers, 1991; Cochard, 1992). The studies give grounds for the supposition that drought stress triggers a nonlinear, spatio-temporal dynamics within the hydraulic network of trees, which may lead to a breakdown of the hydraulic system (Tyree & Ewers, 1991).

The conductivity patterns within tree crowns appear to be a strategy to channel this dynamics (Zimmermann, 1978; 1983). There is also empirical evidence that the stomata respond to conductivity losses (Sperry & Pockman, 1993). The view that stomatal regulation may be tuned to the physical dynamics in the hydraulic network is gradually gaining acceptance (Jones & Sutherland, 1991; Cochard, 1992; Tyree & Cochard, 1996).

A CRITICISM OF THEORETICAL APPROACHES

A theoretical synthesis of empirical observations could clarify how the hydraulic integration of the organism is achieved. The tree water flow models of Running *et al.* (1975), Hatheway & Winter (1981) & Edwards *et al.* (1986) are not suitable for such a synthesis, because the network structure of the hydraulic system is not included. The models of Tyree (1988) and Tyree & Sperry (1988) are the only ones which link functional aspects of the hydraulic system to its branched structure. Up to now, they represent the state-of-the-art in tree water flow modeling. The non-steady-state model of Tyree (1988) is linear, it computes no conductivity losses. The model of Tyree & Sperry (1988) calculates conductivity losses. But as a steady-state model, it does not consider water storage. Water storage and conductivity losses are isolated in specialized models.

Both models share conceptual elements which are considerable steps forward in the theoretical description of the hydraulic system of trees: (1) a locally one-dimensional representation of the hydraulic network and of water flow, and (2) a linkage of functional parameters and algorithms to the structural information based on simple rules. However, these models have shortcomings regarding the separation and transition between the physiological (physical) assumptions and the computational method.

The finite difference model of Tyree (1988) calculates water potential not at the nodes of the space grid, but at the centres of segments between neighbouring nodes. In the case of variable space steps, which are inevitable in the discretization of trees, the distinction between node- and segment-centred difference schemes is significant: segment-centred schemes are not able to approximate consistently the divergence of flow density, which would result as a second-order differential expression from the continuity equation (Manteuffel & White Jr., 1986). Thus, it is to be doubted whether the continuity principle (mass conservation) is reflected by the discrete method. The situation is similiar to Darcy's law. For the flow between neighbouring segment centres, Tyree (1988) does not take into account the conductance at the border between both segments but takes into account the conductance of the segment located downstream. In the case of variable space steps and conductances, the difference expression for the flow is not consistent with the differential expression resulting from Darcy's law.

It is obvious from his text that Tyree (1988) bases the model on mass conservation and Darcy's law. However, no continuous mathematical formulation (differential equation), which would represent the assumptions exactly, is given. Without continuous formulation, the consistency and convergence of the discrete method cannot be evaluated. Thus, the difference equations remain without reference to the underlying physiological assumptions. The final computation results were compared with empirical data. However, from that comparison, probably, no conclusions can be drawn about the validity of assumptions concerning the internal structure and function of the modelled system. In this respect, the model is similiar to a black-box model.

Furthermore, Tyree (1988) uses an explicit difference method, which appears to be simple and comprehensible by intuition. However, it is only

stable if $\Delta t/(\Delta x)^2$ does not exceed a certain threshold at each location of the space grid. A single small space step Δx requires the use of tiny time steps Δt. This involves a high risk that the computational results are dominated by numerical effects, and it is very difficult to achieve a spatial discretization with a uniform accuracy level (Douglas, 1961; Ames, 1977). Consequently, spatial discretization is not subjected to any numerical criteria.

The problems of numerical consistency and convergence are also ignored in the model of Tyree & Sperry (1988). An iterative algorithm is used, apparently to solve a nonlinear boundary value problem. From the view of the authors the iteration loops, which are required until the algorithm converges, reflect real "embolism cycles". During these cycles, a positive feedback would persist between conductivity losses and water potential reduction. But the temporal duration of such cycles can never exceed 0 in any steady-state model. Mixing the properties of the numerical method with physiological reality leads to highly questionable concepts.

THE LEAD OF HYDROLOGY

Tree water flow can be regarded as flow in a porous medium (Siau, 1984) which is spatially organized in a network structure. This is a unique mathematical and physical problem. However, it is akin to the flow problems in soil and groundwater hydrology, which deal also with porous media. The spatially distributed models in hydrology provide a conclusive translation of the physical assumptions by the computational method (Feddes *et al.*, 1988; Istok, 1989). These models represent theories in research (Douglas & Hornung, 1993), and they are applied as technological calculation tools (Abbott & Refsgaard, 1996). Water resources engineering may have contributed to progress in mathematical modeling.

OBJECTIVES OF THE ARTICLE

We present a theoretical framework which is intended to advance the theory of the hydraulic system of trees. The theoretical description takes the form of a numerical simulation model of tree water flow. We try to separate (1) the underlying assumptions about structure and function of the hydraulic system, (2) the discrete formalism, and (3) the simulation software. We attempt to increase universality by the integration of different phenomena, and we are further guided by the principles of falsifiability, simplicity and internal consistency (Munz, 1985).

Including elements of Tyree's (1988) approach, the numerical simulation model combines the phenomena of Darcy flow, water storage and conductivity losses in the hydraulic network of trees. The discrete formalism is chosen to be as simple as possible. However, the soundness of the numerical method should not be sacrificed for simplicity. Discrete formalism and simulation software should constitute a correct translation of the physiological assumptions and thus ensure the internal consistency of the theory.

The numerical simulation model represents a theory, but it is also designed as a tool for structure–function studies. Tree architecture can be treated as a variable model input. This input can be taken from a tree growth model which is able to generate and vary tree architectures by empirically based growth grammars and which can also process information from the total mapping of individual trees. The tree growth model is expounded in Kurth & Früh (1999).

Basic Assumptions and Simulation Method

PRELIMINARIES

The water uptake by roots depends on the water potential difference between the roots and the soil; conversely, root water uptake triggers strongly nonlinear, spatio-temporal dynamics within the soil (Gardner, 1960). Because of this interdependence, it is not sufficient to treat root water uptake and water flow within roots simply as partial aspects of trees. They have to be modelled together with the water movement in the soil. From the theoretical viewpoint, the soil surface is a border dividing the tree organism into two parts, for which substantially different approaches are required. Lafolie *et al.* (1991) & Doussan *et al.* (1998) presented modeling approaches for the soil–root space. We restrict the spatial domain of the theory to the above-ground tree parts. It does not seem possible to overcome

this division at present, but in future, the theoretical description of the hydraulic system may be completed by a coupling of models for the below- and above-ground domains.

Furthermore, the theory is confined to the net transport of water in the longitudinal direction of branching axes. We will give reasons for this in the course of theoretical derivation. The result will be a locally one-dimensional formulation of water flow, in which the network of flow paths coincides with the network of branching axes.

To assure a transparent transition from the underlying physiological assumptions to the final computation results, we proceed as follows: first, we concentrate on segments of the network with constant cross-section. Such segments are unbranched and thus exhibit no discontinuities of the hydraulic properties. For these segments, the basic assumptions are condensed to a continuous equation. Then we choose a discrete (numerical) method and evaluate its ability to approximate the continuous equation. This enables us to assess whether the basic assumptions are translated correctly by the discrete method. Finally, including specific properties of the branched structure, the discrete formulation is extended to the entire network.

BASIC QUANTITIES

The fundamental measure to describe water transport in trees is the water potential Ψ(Pa), which quantifies the free energy per unit volume of an aqueous phase (Slatyer, 1967; Mohr & Schopfer, 1993). Water flows spontaneously along falling gradients of Ψ. Within plants, Ψ is a sum of different components. Assuming that temporal and spatial changes of the osmotic pressure and the matric potential are without importance for long-distance water transport,

$$\Psi = P + \varrho_{H_2O}\, g\, z \tag{1}$$

is valid, where P is the hydrostatic pressure (Pa); $\varrho_{H_2O}\, g\, z$ is the gravitational potential (Pa), ϱ_{H_2O} being the density of water, g the gravitational acceleration, and z the height over a reference level. The xylem as the water-conducting tissue of trees exhibits the essential properties of a porous medium (Siau, 1984). Thus, the relation between the Ψ-gradient and the mass flow F(kg s^{-1}) can be specified by Darcy's law,

$$F = \hat{K}\,\frac{\partial \Psi}{\partial x} \tag{2}$$

where $\hat{K}$ is the hydraulic conductivity normalized by length (kg s^{-1} MPa^{-1} m). Darcy's law provides a natural measuring instruction for $\hat{K}$, e.g. the gravity flow method (Zimmermann, 1978). All methods integrate over the total volume of the sample piece and thus yield a spatially effective value of $\hat{K}$. For flow in the longitudinal direction of woody axes, $\hat{K}$ is interpreted as axial conductivity.

If shoot axes are cleared of xylem embolism by pressure flushing (Sperry *et al.*, 1988) and are subsequently subjected to progressive dehydration, the decline of conductivity with pressure or water content can be quantified by *vulnerability curves* (Tyree & Sperry, 1989; Sperry & Tyree, 1990; Cochard, 1992). The curves generally follow

$$1 - \frac{\hat{K}(P(t))}{\hat{K}(0)} = \not{f}(P(t)) \tag{3}$$

where $\hat{K}(0)$ is the maximal conductivity at the beginning of the experiment and $\not{f}(P(t))$ is a function depending on species.

Studies by Milburn (1979), Petty & Palin (1983), Sperry *et al.* (1987), Katz *et al.* (1989) and Borghetti *et al.* (1991) give a complex picture from which we may extract a basic pattern. The reversal of conductivity losses seems to be bound to specific conditions and to be slower than the formation. We assume complete irreversibility as approximation of reality.

The notation $\hat{K}(P)$ does not mean a function in a strict mathematical sense, since the relation from P to $\hat{K}$ is in general not unique. $\hat{K}$ is rather a product of the history of the tree. A solution to this problem will be given with the discrete formulation.

The hydraulic capacitance c (kg dm^{-3} MPa^{-1}) quantifies the ability of tree organs to store or release water with isothermal Ψ-changes:

$$c(P) = \frac{\partial \theta}{\partial \Psi} \tag{4}$$

where θ is the water content (kg dm^{-3}). For leaves and shoot axes, c often is calculated from the slope of dehydration isotherms obtained by different methods (Waring *et al.*, 1979; Edwards & Jarvis, 1982; Tyree *et al.*, 1983; Tyree & Yang, 1990). As with the measurement of $\hat{K}$, the methods yield spatially integrated results.

ASSUMPTION OF SPATIAL HOMOGENEITY OF CAPACITANCE AND AXIAL CONDUCTIVITY

The theoretical synthesis of the hydraulic system should correspond to an appropriate empirical analysis: the tree has to be broken down into sample pieces in such a way that their material properties can be measured under well-defined boundary conditions. In this sense, leaves or leaf blades are useful subunits for the measurement of capacitance. A second type of useful subunit, which we call *axis segment*, is obtained if the network of branching axes is cut perpendicularly to the axial direction into unbranched pieces with homogeneous diameters. For axis segments with their geometrically clear boundaries, spatially effective values of capacitance and axial conductivity can be measured. Homogeneous diameters (d) are needed, since $\hat{K}$ increases nonlinearly with d (see below). The network of flow paths can be reconstructed from axis segments, and the flow dynamics can be computed on the basis of measured hydraulic properties of the segments. This way of theoretical synthesis requires the assumption that within axis segments, capacitance and axial conductivity are superimposed in a spatially homogeneous manner.

The subdivision into bark and wood, and within the xylem cylinder, the differentiation between inner and outer sapwood, parenchymatic and tracheidal/tracheal tissue, late and early wood, indicate a spatial separation of capacitive and conductive functions. This may have consequences for hydraulic leaf–root signalling. Deliberating on this, Weatherley (1970) and Jarvis (1975) assumed a division into axial conduction and lateral storage connected by transfer resistances. They inferred a rapid axial and a slow lateral signalling without quantifying the dynamics in more detail. However, a quantitative derivation of system dynamics from structure can neither be empirically based nor tested if the conductor–capacitor separation is the premise. With the exception of the wood–bark relationship, the geometrical relations between capacitive and conductive elements are highly complex (Braun, 1970; Wilson & White, 1986). Furthermore, cavitation and refilling of conduits may cause transitions between both elements (Waring *et al.*, 1979; Tyree & Yang, 1990; Borghetti *et al.*, 1991).

In contrast, modeling based on the assumption of homogeneity substantially increases falsifiability (a theory may be more or less falsifiable; see Munz, 1985). The structure of the system can be modelled on measured data, as it is possible to test the computed system dynamics by spatially integrating measurements, e.g. flow measurements by the heat balance method (Čermák *et al.*, 1976; Kučera *et al.*, 1977; Schulze *et al.*, 1985; Granier, 1987).

CONTINUOUS WATER FLOW EQUATION FOR REGIONS WITH CONSTANT CROSS-SECTION

We add a further principle and complete the trinity of basic assumptions: (1) mass conservation, (2) Darcy's law, and (3) spatial homogeneity of capacitance and axial conductivity. The mathematical expression of mass conservation is the one-dimensional continuity equation

$$\frac{\partial f}{\partial x} = -\frac{\partial \theta}{\partial t} \tag{5}$$

where f is the flux density (kg s^{-1} m^{-2}). Applying Darcy's law and the assumption of homogeneity by substituting eqns (2) and (4) into eqn (5) with K as hydraulic conductance (kg s^{-1} MPa^{-1} m^{-1}), and adding the sink term $E(t)\ell(x)$ for the transpiration, we get

$$\frac{\partial}{\partial x}\left[K(x, P)\,\frac{\partial \Psi}{\partial x}\right] = c(x, P)\,\frac{\partial \Psi}{\partial t} + E(t)\,\ell(x) \tag{6}$$

where $E(t)$ is the transpiration flux density (kg $s^{-1} m^{-2}$), and $\ell(x)$ the local leaf area (m^2 m^{-3}) with a formal reference to the axis volume which can be dropped in the discrete formulation.

Equation (6) involves the following simplifications: Leaf areas are assigned as transpirational

surfaces to the axis segments, and the leaf capacities are added to the segment capacities. This implies a uniform distribution of leaf area over the surface of the segments, which appears appropriate for conifers. Furthermore, the transfer resistances between leaf capacities and shoot axes are neglected. However, in deciduous trees, transfer resistances can be significant (Yang & Tyree, 1994), and the series of leaf capacity and transfer resistance can contribute to system dynamics (Landsberg *et al*., 1976). We argue that representing the leaves as individual compartments diminishes falsifiability. Without affecting the theoretical derivation, the contribution to system dynamics can be included by a low-pass filtering of transpiration. The problem requires an adequate comparison between simulated and measured dynamics, which is beyond the scope of this article.

Further simplifications concern the integration of trees within the soil–plant–atmosphere continuum: as a model input, transpiration flux density is not spatially variable, and stomatal control is not included. The theoretical framework can be supplemented also by these aspects without substantial change (see below).

Equation (6) is a member of the family of nonlinear diffusion equations. With initial and boundary conditions, an initial boundary value problem (IBVP) results, which defines a unique spatio-temporal dynamics. We will specify the conditions when we extend the formulation to the entire network.

DISCRETE APPROXIMATION OF THE CONTINUOUS FLOW EQUATION

Nonlinear IBVPs involving eqn (6) belong to a type of problem to which the finite difference method of Douglas & Jones (1963) applies. This is a Crank–Nicholson scheme linearized by a predictor–corrector method. Using equidistant spatial (Δx) and temporal (Δt) steps, it converges with $O[(\Delta x)^2 + (\Delta t)^{3/2}]$. The method is unconditionally stable. Von Rosenberg (1969) introduced a simplification, which decreases computing demand and probably increases accuracy. It was shown that this simplification also applies to tree water flow (Früh, 1995). For the general case of variable step-widths, the notation for the grid points (x_j, t_n) is

$$x_{j+1} = x_j + \Delta x_{j+1}, \qquad t_{n+1} = t_n + \Delta t_{n+1}.$$

Intermediate locations in space are explained as

$$x_{j+1/2} = x_j + \tfrac{1}{2}\Delta x_{j+1}, \qquad x_{j-1/2} = x_{j-1} + \tfrac{1}{2}\Delta x_j$$

and correspondingly for time. Let $\Psi_{j,n}$ denote $\Psi(x_j, t_n)$, and for the arithmetic mean of the pressures at neighbouring space points

$$P_{j+1/2,n} := \frac{P_{j,n} + P_{j+1,n}}{2}$$

$$P_{j-1/2,n} := \frac{P_{j-1,n} + P_{j,n}}{2}$$

while the vulnerable conductance is always calculated at the midpoint between neighbouring space points:

$$K_{j+1/2,n} := K(x_{j+1/2}, P_{j+1/2,n})$$

$$K_{j-1/2,n} := K(x_{j-1/2}, P_{j-1/2,n})$$

The host of indices cannot be dispensed with, since careful centreing of variables is crucial for the consistency of the discrete with the continuous formulation (Douglas & Jones, 1963; Von Rosenberg, 1969; Ames, 1977; see also introduction). Using the difference operators

$$D_x^+ \Psi_{j,n} := \frac{\Psi_{j+1,n} - \Psi_{j,n}}{\Delta x_{j+1}}$$

$$D_x^- \Psi_{j,n} := \frac{\Psi_{j,n} - \Psi_{j-1,n}}{\Delta x_j}$$

the finite difference method adapted to eqn (6) is

Predictor equation:

$$\frac{K_{j+1/2,n} D_x^+ \Psi_{j,n+1/2} - K_{j-1/2,n} D_x^- \Psi_{j,n+1/2}}{\tfrac{1}{2}(\Delta x_j + \Delta x_{j+1})} = c_{j,n} \frac{\Psi_{j,n+1/2} - \Psi_{j,n}}{\tfrac{1}{2}\Delta t} + E_n \ell_j \qquad (7a)$$

Corrector equation:

$$\frac{K_{j+1/2,n+1/2}\,\frac{1}{2}[D_x^+\Psi_{j,n+1}+D_x^+\Psi_{j,n}]-K_{j-1/2,n+1/2}\,\frac{1}{2}[D_x^-\Psi_{j,n+1}+D_x^-\Psi_{j,n}]}{\frac{1}{2}(\Delta x_j+\Delta x_{j+1})}$$

$$=c_{j,n+1/2}\frac{\Psi_{j,n+1}-\Psi_{j,n}}{\Delta t}+E_{n+1/2}\,\ell_j \tag{7b}$$

After each solution of eqns (7a) and (7b), K, c and E are updated. Since we assume irreversibility of conductance losses, a fixed function table, as in hydrological modeling (Istok, 1989), cannot be used for K. The new K has to be developed from the old K using the derivation of the vulnerability function $\not\in(P(t))$ from eqn (3). We choose a Runge–Kutta method and update K only when pressure declines.

Updating K after predictor:

$$K_{j+1/2,n+1/2}=\begin{cases}K_{j+1/2,n}\\ \qquad \text{if } (P_{j+1/2,n+1/2}-P_{j+1/2,n})\geqslant 0,\\ K_{j+1/2,n}-K_{j+1/2,0}\,\dfrac{\mathrm{d}}{\mathrm{d}P}\not\in\left(\dfrac{P_{j+1/2,n}+P_{j+1/2,n+1/2}}{2}\right)(P_{j+1/2,n+1/2}-P_{j+1/2,n})\\ \qquad \text{else}\end{cases} \tag{8a}$$

for $K_{j-1/2,n+1/2}$ correspondingly;

Updating K after corrector:

$$K_{j+1/2,n+1}=\begin{cases}K_{j+1/2,n}\\ \qquad \text{if } (P_{j+1/2,n+1}-P_{j+1/2,n})\geqslant 0,\\ K_{j+1/2,n}-K_{j+1/2,0}\,\dfrac{\mathrm{d}}{\mathrm{d}P}\not\in\left(\dfrac{P_{j+1/2,n}+P_{j+1/2,n+1}}{2}\right)(P_{j+1/2,n+1}-P_{j+1/2,n})\\ \qquad \text{else}\end{cases} \tag{8b}$$

and for $K_{j-1/2,n+1}$ correspondingly.

EXTENSION OF THE DISCRETE FLOW EQUATIONS TO VARIABLE CROSS-SECTIONS

To prepare the extension of the discrete method to the entire hydraulic network with variable cross-sections and branchings, we remove the temporal discretization. Equations (7a) and (7b) unify into

$$\frac{K_{j+1/2}\,D_x^+\Psi_j-K_{j-1/2}\,D_x^-\Psi_j}{\frac{1}{2}(\Delta x_j+\Delta x_{j+1})}=c_j\left.\frac{\partial\Psi}{\partial t}\right|_j+E\ell_j.$$

We turn to a region of the network still without branchings but with changing cross-sections (Fig. 1). Using the relation between K and $\hat{K}$ with A as cross-section leads to

$$\frac{1}{A_{j+1/2}}\hat{K}_{j+1/2}\,D_x^+\,\Psi_j-\frac{1}{A_{j-1/2}}\hat{K}_{j-1/2}\,D_x^-\Psi_j$$

$$=\left[c_j\left.\frac{\partial\Psi}{\partial t}\right|_j+E\ell_j\right]\frac{1}{2}(\Delta x_j+\Delta x_{j+1}) \tag{9}$$

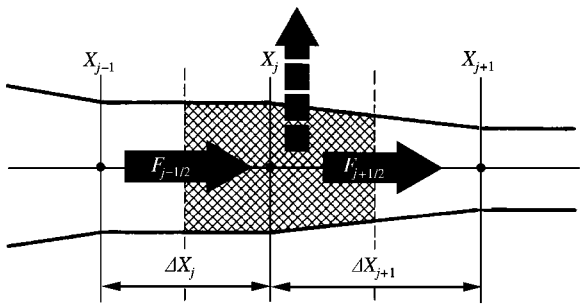

FIG. 1. Spatial discretization scheme for an unbranched part of the hydraulic network with variable cross sections. The shaded region, which is composed of segment halves joining at the grid point x_j, represents the cell for which mass conservation is valid according to eqn (10). Arrows indicate flows across the borders of the cell and transpirational water loss.

where $\hat{K}_{j+1/2} D_x^+ \Psi_j = F_{j+1/2}$ and $\hat{K}_{j-1/2} D_x^- \Psi_j = F_{j-1/2}$ are discrete Darcy formulations for influx and outflux of the shaded cell in Fig. 1. In general, the difference between influx and outflux is not balanced by the change of water content and the transpirational water loss of the cell. The condition of mass conservation is only fulfilled if $A_{j+1/2} = A_{j-1/2}$, that is, if the cross-section is constant within the interval $[j-1, j+1]$. However, we retain this fundamental principle and replace eqn (9) by

$$\hat{K}_{j+1/2} D_x^+ \Psi_j - \hat{K}_{j-1/2} D_x^- \Psi_j = \left[c_j \left. \frac{\partial \Psi}{\partial t} \right|_j + E\ell_j \right] \times \frac{1}{2} (\Delta x_j A_{j-1/2} + \Delta x_{j+1} A_{j+1/2}) \qquad (10)$$

where $\frac{1}{2} (\Delta x_j A_{j-1/2} + \Delta x_{j+1} A_{j+1/2})$ is conceived as a discrete approximation of the cell volume. The convergence of the discrete solution to the solution of differential equation (6) is probably impaired by the replacement. The convergence is only ensured in the limit case of constant cross-section, i.e. locally. Equation (10) then becomes identical to eqn (9).

Differential equations of the same type as eqn (6) are used for modeling of soil water movement (Feddes *et al.*, 1988; Istok, 1989). We have to move away slightly from the reference to eqn (6) because of a substantial difference between soil and tree. For the flux densities and the reference volumes of water content, uniform cross-sections are pre-supposed in the soil. They are never mentioned explicitly in formulae. In contrast, the tubular elements of the hydraulic network of trees are sharply delimited from the environment and are characterized by variable geometrical quantities.

EXTENSION TO BRANCHINGS

The discrete conservation equation (10) is now extended to the case where a spatial grid point is a branching node as well, and where, as a result, the cell of mass conservation consists of more than two segment halves (Fig. 2). The discrete approximation of the cell volume is

$$\Delta V_j = \frac{1}{2} \left(A_{j-1/2} \Delta x_j + \sum_v A^v_{j+1/2} \Delta x^v_{j+1} \right)$$

with the superior index v, to distinguish the segments following the branching node. We dispense with the difference operators and usethe non-normalized conductivity $\tilde{K}$ instead of $\hat{K}$. We further proceed from c_j and ℓ_j to the capacity C_j and leaf area L_j for a cell of given volume. Then the discrete conservation equation

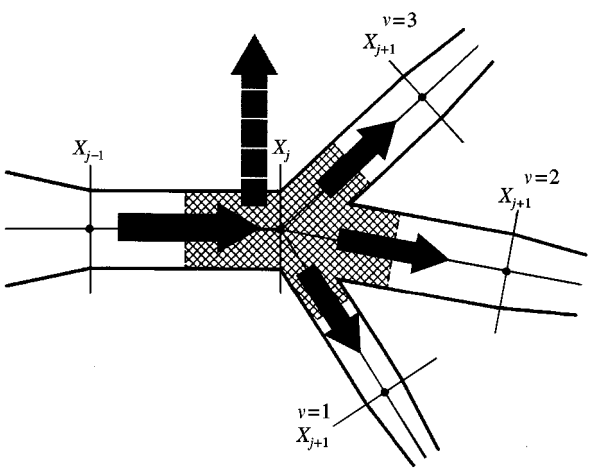

FIG. 2. Spatial discretization scheme in the vicinity of a branching node. For the shaded cell bordered by the midpoints of segments joining at x_j, mass conservation is valid according to eqn (11).

including branching is

$$\sum_v \tilde{K}^v_{j+1/2}(\Psi^v_{j+1}-\Psi_j)-\tilde{K}_{j-1/2}(\Psi_j-\Psi_{j-1}) = C_j\left.\frac{\partial\Psi}{\partial t}\right|_j + EL_j \quad (11)$$

which is attractive in its simplicity.

DISCRETE IBVP FOR TREE WATER FLOW

We now reintroduce the temporal discretization of the difference method (7a,b) into eqn. (11) and specify the initial and boundary conditions. This results in the discrete IBVP which will be the basis for the numerical simulation of water flow in the branched tree architecture:

Predictor:

$$\sum_v \tilde{K}^v_{j+1/2,n}(\Psi^v_{j+1,n+1/2}-\Psi_{j,n+1/2}) - \tilde{K}_{j-1/2,n}(\Psi_{j,n+1/2}-\Psi_{j-1,n+1/2}) = C_{j,n}\frac{\Psi_{j,n+1/2}-\Psi_{j,n}}{\frac{1}{2}\Delta t} + E_nL_j \quad (12a)$$

Corrector:

$$\sum_v \tilde{K}^v_{j+1/2,n+1/2}\frac{1}{2}(\Psi^v_{j+1,n+1}-\Psi_{j,n+1}+\Psi^v_{j+1,n}-\Psi_{j,n}) -\tilde{K}_{j-1/2,n+1/2}\frac{1}{2}(\Psi_{j,n+1}-\Psi_{j-1,n+1}+\Psi_{j,n}-\Psi_{j-1,n}) = C_{j,n+1/2}\frac{\Psi_{j,n+1}-\Psi_{j,n}}{\Delta t} + E_{n+1/2}L_j \quad (12b)$$

Boundary condition:

$$\Psi_{j=0,n} = \Psi_{soil} \quad (12c)$$

Initial condition:

$$\Psi_{j,n=0} = \Psi_{soil}$$

$$P_{j,n=0} = \Psi_{soil} - \varrho_{H_2O}\, g\, z_j \quad (12d)$$

Note: Conductivity is updated with pressure according to eqns (8a,b).

Boundary condition (12c) reflects that the soil is not included in the spatial domain of the theory but forms the domain border. It is represented as the lowest point of the space grid (in the difference equations indexed by $j = 0$). Starting with the trunk base, all succeeding points belong to the tree ($j > 0$). Since the transpiration is written as a sink term, the boundary condition is one-sided. Thermodynamic equilibrium is chosen as the initial state (12d). From eqn (1) the formulation for pressure resulted, which is often used for pre-dawn potentials (e.g. Ritchie & Hinckley, 1975). Finally, it should be noted that, by treating E also as a function of x and Ψ, spatially variable transpiration flux densities and the stomatal control can be included without change of the discrete IBVP.

PARAMETRIZATION OF THE IBVP

For the parametrization of the IBVP (12) a principle of Tyree (1988) is applied, which derives the local hydraulic properties from local geometry. The principle makes the adaptation of functional information simple when the structural data are exchanged. It facilitates structure–function studies which treat tree architecture as independent variable. The applicability of the parametrization principle is based on the assumption of homogeneity introduced above. Appropriately, the parametrization is carried out during calculation of the initial state:

Conductivity: The initial conductivity is given solely by xylem microanatomy and is not impaired by any embolism. The initial local $\tilde{K}$ values are calculated from empirical regressions between $\hat{K}$ and the axis diameter d (Tyree, 1988; Cochard, 1992). The centred conductivities

needed in eqn (12) are

$$\tilde{K}_{j+1/2,n=0} = \frac{\alpha\,(d_{j+1/2})^{\beta}}{\Delta x_{j+1}} \qquad (13)$$

for $\tilde{K}_{j-1/2}$ correspondingly, where α and β ($2.0 < \beta < 3.0$) and α are coefficients depending on species.

Capacity: In eqn (12), the capacity $C_{j,n}$ of the cell of mass conservation results from summing up the capacities of segment halves joining at x_j:

$$C_{j,n} := \frac{1}{2}\left(C_{j-1/2,n} + \sum_{v} C^{v}_{j+1/2,n}\right) \qquad (14)$$

The capacities of segment halves in turn are obtained from the component ${}^{a}C$ of the shoot axis volume and the component ${}^{\ell}C$ of the attributed leaf area. The initial local capacities are coupled to axis volumes and leaf areas by capacitances:

$$C_{j+1/2,n=0} = \tfrac{1}{2}\,({}^{a}c_{j+1/2,n=0}\,A_{j+1/2}\,\Delta x_{j+1} + {}^{\ell}c_{j+1/2,n=0} L_{j+1/2}) \qquad (15)$$

where $L_{j+1/2}$ is the leaf area of the segment Δx_{j+1}. Equation (15) analogously holds true for $C_{j-1/2,n=0}$.

For the simulations presented here, tree structures of *Picea abies* and *Thuja occidentalis* were used and parametrized as follows: For *P. abies* $\alpha = 5.370 \times 10^{-5}\,\mathrm{kg\,s^{-1}\,MPa^{-1}\,m}$ and $\beta = 2.44$ were taken from Cochard (1992), and for *T. occidentalis*, $\alpha = 2.477 \times 10^{5}\,\mathrm{kg\,s^{-1}\,MPa^{-1}\,m}$ and $\beta = 2.52$ from Tyree (1988). For *P. abies* and *T. occidentalis*, ${}^{a}c = 0.1\,\mathrm{kg\,dm^{-3}\,MPa^{-1}}$ and ${}^{\ell}c = 0.04\,\mathrm{kg\,m^{-2}\,MPa^{-1}}$ were taken from Tyree (1988) and provisionally treated as constants. We approximated the vulnerability curves of Cochard (1992) and Sperry & Tyree (1990) by logistic functions ${}^{\ell}f(P) = 1/(1 + e^{b(P - P_{V50})})$ with $b = 2.42\,\mathrm{MPa^{-1}}$ and $P_{V50} = -3.52\,\mathrm{MPa}$ for *P. abies* and $b = 1.72\,\mathrm{MPa^{-1}}$ and $P_{V50} = -3.55\,\mathrm{MPa}$ for *T. occidentalis*.

SOLUTION OF THE LINEAR SETS OF EQUATIONS

The predictor and corrector equation in the IBVP (12) each represent a linear set of equations. Thus two linear sets are to be solved per time step, and the number J of equations equals the number of spatial grid points. A Cholesky algorithm is used for the solution of the linear sets. Its count of floating point operations normally increases with J^3 (Press *et al.*, 1992). However, we were able to tailor the algorithm to the specific problem so that the operation count increases only with J. This adjustment is crucial for the practicability of network modeling, because J usually is between 10^4 and 10^5.

SPATIAL DISCRETIZATION BY NATURE AND NUMERICAL CRITERIA

The branching points and the end points of branching axes determine a highly variable and random distance pattern. It is a discretization given by nature. To obtain a discrete method with sufficient accuracy and efficiency, the discretization has to fulfil two numerical criteria:

(I) *Uniform accuracy*: The spatial steps have to be large where moderate gradients develop, and small where the gradients are steep (Lapidus & Pinder, 1982). Alternatively, the smallest distance required in the tree could be chosen as universal grid spacing. However, this is discarded for reasons of computational economy.

(II) *Locally limited variation of step-widths*: This helps to prevent the reduction of convergence order which normally accompanies the transition from constant to variable spacing (Manteuffel & White Jr., 1986; Grossmann & Roos, 1992). In general, truncation error terms of order $O[\Delta x_{j+1} - \Delta x_j]$ become bounded.

Evidently, only a compromise between both requirements can be realized. Furthermore, the water potential gradients in the hydraulic network may vary by up to three orders of magnitude (Tyree & Ewers, 1991), and no correlation is known between the spatial pattern of gradients and the spacing given by branching and terminal nodes. Since the locations of these grid points are more or less fixed, the room for setting points due to numerical requirements is markedly constricted in contrast to ordinary discretization problems (e.g. Trompert & Verwer, 1990). The network spacing is a handicap impeding numerical discretization. However, within the given

framework we can utilize a wide range of distances to follow criteria (I) and (II), since we are not restricted by a numerical stability condition (see introduction).

Criteria (I) and (II) guarantee accuracy independently of structural peculiarities. This standardization is essential, if we want to study how hydraulic function depends on tree architecture. Therefore, a discretization algorithm forms a natural interface between hydraulic and architectural modelling.

DISCRETIZATION AS A LINK BETWEEN STRUCTURAL AND FUNCTIONAL MODELLING

The multi-step discretization algorithm starts with a *base grid*. Except the trunk below the crown base, it contains only branching and terminal nodes as grid points. The final product is called a *hydraulic map* following Tyree (1988). Both base grid and hydraulic map are stored as lists of nodes in a data format similar to the maps of Tyree (1988). The individual node number together with the numbers of the neighbour nodes gives the topological information. This is supplemented by the geometrical data (length, diameter, leaf area) of the segment which joins the node to its proximal neighbour.

While the hydraulic map is the input of the hydraulic model, the base grid is delivered by the architectural model GROGRA (Kurth & Früh, 1999). It can generate the base grid format from two different sources:

(1) Information from the total mapping of individual trees. In this way, the data of the *T. occidentalis* tree (mapped by Tyree, 1988) and of some *P. abies* trees (sample C in Kurth and Früh, 1999) were made accessible to discretization.

(2) Tree structures which GROGRA modelled by empirically based growth grammars. Here, empirical information is used in a more processed and generalized form (Kurth & Früh, 1999).

To approximate criterion (I), we utilize the fact that the leaf-specific conductivity $LSC_{j-1/2}$ between two grid points is inversely proportional to the steady-state Ψ-gradient (Zimmermann, 1978; Tyree *et al.*, 1983). Given a certain E, $LSC_{j-1/2} = E(\Delta x_j/\Delta\Psi_{j,stat})$ is valid. Scaling the accuracy level by a global factor G, the so-called criterion distances $CD_j = LSC_{j-1/2}\,G$ are calculated, which vary in space. If the lengths Δx_j were replaced by CD_j, at steady state, the same Ψ-difference $\Delta\Psi_{j,stat} = \Delta\Psi^E_{stat} = EG$ would drop along all segments of the tree. We call $\Delta\Psi^E_{stat}$ the steady-state accuracy level with the given E.

Three transformation steps follow: (1) By shifting and fusing of nodes, segments are removed from the base grid if their lengths Δx_j are small compared to their criterion distances CD_j (for details see Kurth, 1994). (2) The segments are subdivided equidistantly by intermediate segments. Their number is calculated from rounding off $\Delta x_j/CD_j$. (3) By an iterative shifting of the intermediate nodes, the spatial variation of step-widths is smoothened until the desired compromise between criteria (I) and (II) is realized. Finally, we obtain the hydraulic map, which can be used for simulation. For more details see Früh (1995).

TEMPORAL DISCRETIZATION

In contrast to the space domain, no grid points are fixed *a priori* within the time domain. With regard to temporal discretization, tree water flow does not seem to be unusual in the class of IBVPs. Thus, an algorithm was taken from Hornung & Messing (1984), which adjusts time steps such that the change of water content θ per step approximates a desired optimum $\Delta\theta_{opt}$, where a halving of $\Delta\theta_{opt}$ on average leads to a halving of time steps.

Model Tests

The convergence property of the finite difference method of Douglas & Jones (1963) is mathematically proven. But on the way up to IBVP (12), several adjustments were made, and the computer program HYDRA mediates between the IBVP and the final simulation results. Model tests should give additional evidence that the physical and physiological assumptions are translated correctly. Steps or rectangles of transpiration flux density were often given as input signals in the model tests. The signals change

between the zero level and 5.0×10^{-6} kg s^{-1} m^{-2}, a normal daily transpiration maximum of *P. abies*. We prefer this signal type for two reasons: it is a hard endurance test of the numerical method, and the step response characterizes the linear system behaviour comprehensively (see below).

SPATIAL CONVERGENCE

In the *P. abies* growth grammar of Kurth & Früh (1999), stochastic variations were eliminated and the lengths of branching axes extended by a factor of 1.5. A 4-year-old tree was generated from the grammar and transformed to a base grid. It served as the common ancestor for the generation of four hydraulic maps differing from each other only in terms of spatial discretization, while the branching and terminal nodes are identical. For the four maps, the steady-state accuracy levels $\Delta\Psi^{E}_{stat} = 4.0 \times 10^{-3}$, 2.0×10^{-3}, 1.0×10^{-3} and 5.0×10^{-4} MPa were chosen, which in the mean corresponds to a progressive halving of spatial steps. The control parameter $\Delta\theta_{opt}$ for temporal discretization was set to 10^{-4} kg dm^{-3}, Ψ_{soil} was 0.0 MPa, the initial condition as in eqn (12d), E was a rectangle signal with a breadth of 1 h located within a total time interval of 2 h.

We found that with each halving of space steps the relative Ψ-differences stay within 4% at the half-times of responses (ca. 3 min after step-wise changes), and within 0.2%, when the steady-state flow maxima are reached. The differences did not change significantly from the first to the third halving of steps.

TEMPORAL CONVERGENCE

From the trees in the tests for spatial convergence, the hydraulic map with the accuracy level $\Delta\Psi^{E}_{stat} = 10^{-3}$ MPa for $E = 5.0 \times 10^{-6}$ kg s^{-1} m^{-2} was taken. Four simulations were run with $\Delta\theta_{opt} = 10^{-3}$, 5×10^{-4}, 10^{-4}, 10^{-5} kg dm^{-3}. In the mean this approximately corresponds to a progressive halving of time steps, which however may change during an individual simulation by three to four orders of magnitude. Transpiration, total time interval, and initial and boundary conditions were set as in the tests for spatial convergence.

We found that with each halving of time steps the relative Ψ-differences stay within 2% at the half-times of responses and within 0.01% when the steady-state flow maxima are reached. The differences did not vary significantly from the first to the third halving of steps.

ROUTINE CHECKING OF MASS BALANCE

During each simulation, HYDRA automatically generates a protocol of mass balance, in which for individual time steps the input–output balance of the tree is compared with its internal mass change. Independently of tree architecture and course of transpiration, the differences observed never exceeded the order of machine accuracy (2.2×10^{-16}). The simulation protocols also confirm that at steady state the input–output balance and the internal mass change equal 0 (within the scope of machine accuracy).

SENSITIVITY TO CHANGES OF CONDUCTIVITY, CAPACITY AND LEAF AREA

By the *P. abies* growth grammar (Kurth & Früh, 1999), a 15-year-old model spruce was generated and transformed to a hydraulic map. It served as a control tree with leaf areas given by the grammar, and conductivities and capacities following the data in the parametrization section. By global scaling factors of 2.0 and 0.5, six tree variants were generated which differed in the levels of one of the three properties of conductivity, capacity and leaf area. The accuracy level $\Delta\Psi^{E}_{stat}$ of all test trees was within 4.0×10^{-3} MPa, and the control parameter $\Delta\theta_{opt}$ was set to 10^{-4} kg dm^{-3}. Ψ_{soil} was 0.0 MPa, as initial condition thermodynamic equilibrium was chosen. At the starting time, E changed step-wise from 0 to 5×10^{-6} kg s^{-1} m^{-2}; the total time interval was 7 h. The step response of flow at the trunk base was used to characterize the system behaviour of the test trees.

We found that a doubling of one of the three quantities $1/\tilde{K}$, C, L raised half-times by factors < 3.0, while the halving of a quantity reduced half-times by factors > 0.4.

NUMERICAL STABILITY

The same hydraulic map was used as in the tests for temporal convergence. The control

parameter $\Delta\theta_{opt}$ for temporal discretization was set to 10^{-4}. Ψ_{soil} was 0.0 MPa. For the stability tests, perturbation terms were superimposed on the initial condition (12d), which normally should assign Ψ_{soil} to all spatial grid points: $\Psi_{j,n=0} = \Psi_{soil} + a \cdot r_j(-1.0, 1.0)$, where the function $r_j(-1.0, 1.0)$ generates random numbers evenly distributed within the interval $[-1.0, 1.0]$ and a is the perturbation amplitude. At starting time, E changed step-wise from 0 to 5×10^{-6} kg s^{-1} m^{-2}; the total time interval was 2 h.

The simulated potentials were compared with the results of a non-perturbed simulation. The total Ψ-range covered during simulations was about 4×10^{-2} MPa. A perturbation amplitude $a = 5 \times 10^{-3}$ MPa was dampened to fractions between 6 and 1% at the half-time of step response (ca. 3 min after start of simulation), and at the steady-state end of simulations to fractions between 2.5 and 0.025%. Perturbations with $a > 5 \times 10^{-3}$ MPa decayed only incompletely, which can be traced back to irreversible conductivity losses.

A POSTERIORI ERROR ANALYSES

With the test simulations for numerical stability, *a posteriori* error analyses (Watkins, 1991) were carried out to evaluate how accurately the linear sets of equations in the IBVP (12) are solved. The analyses revealed that the residuum of the predictor set [eqn (12a)] as well as of the corrector set [eqn (12b)] does not exceed machine accuracy (2.2×10^{-16}) by more than one order of magnitude.

DISCUSSION OF TEST RESULTS

From the tests for spatial and temporal convergence we conclude that $\Delta\Psi^E_{stat} \leqslant 4.0 \times 10^{-3}$ MPa and $\Delta\theta_{opt} \leqslant 10^{-3}$ kg dm^{-3} are scopes of the control parameters of step widths appropriate for simulation, because finer discretizations lead to no significant change in the solution function. Mass conservation within the limits of machine accuracy is a consequence of the conservative difference eqn (11) and not a matter of course: finite element models of groundwater or soil hydrology may exhibit deviations from mass conservation up to several percents (Istok, 1989). The rapid decay of perturbations superimposed on the initial state points to a high numerical stability of the model and thus reproducibility of the results. The tests for sensitivity and stability indicate that the matrices of the linear sets of equations given by eqns (12a) and (12b) have a small condition number (Watkins, 1991). Thus, we can interpret the tiny residual of the error analyses as due to the effect that the accuracy of the computed solutions is limited only by round-off errors due to computer hardware. Summarizing, the test results give strong evidence that the computational translation of the physical and physiological assumptions is reproducible and sufficiently exact.

Simulation Studies

STEADY-STATE WATER POTENTIAL PROFILES OF *PICEA ABIES* AND *THUJA OCCIDENTALIS*

The steady-state water potential profiles of the following trees were studied: of a 15-year-old model spruce generated by the *P. abies* growth grammar (Kurth & Früh, 1999), of a mapped 12-year-old *P. abies* tree (sample C in Kurth & Früh, 1999) and of a 10 m high *T. occidentalis* tree mapped by Tyree (1988), who also investigated its hydraulic properties. Water flow was simulated linearly, that is without conductivity losses. $\Delta\Psi^E_{stat}$ of the trees was within 4.0×10^{-3} MPa, $\Delta\theta_{opt}$ was set to 10^{-4} kg dm^{-3}. Ψ_{soil} was 0.0 MPa, thermodynamic equilibrium was chosen as the initial condition. At starting time, E changed step-wise from 0 to 5×10^{-6} kg s^{-1} m^{-2}; the total time interval was 7 h. To generate the profiles from the simulation results, we picked a time when steady state was reached. For the display of flow paths, we selected the tree trunk and at least 20 first-order axes branching off the trunk at approximately equal distances (Fig. 3).

We found in all the three trees that the water potentials of the branches on average drop steeper than the potentials of the trunk. As a consequence, the branch tips have a markedly lower potential than trunk points at the same path length (Fig. 3). In the mapped as well as in the modelled spruce, the gradients of trunk and branches decline towards the ends of the axes, where they hardly exceed the gradient of gravity

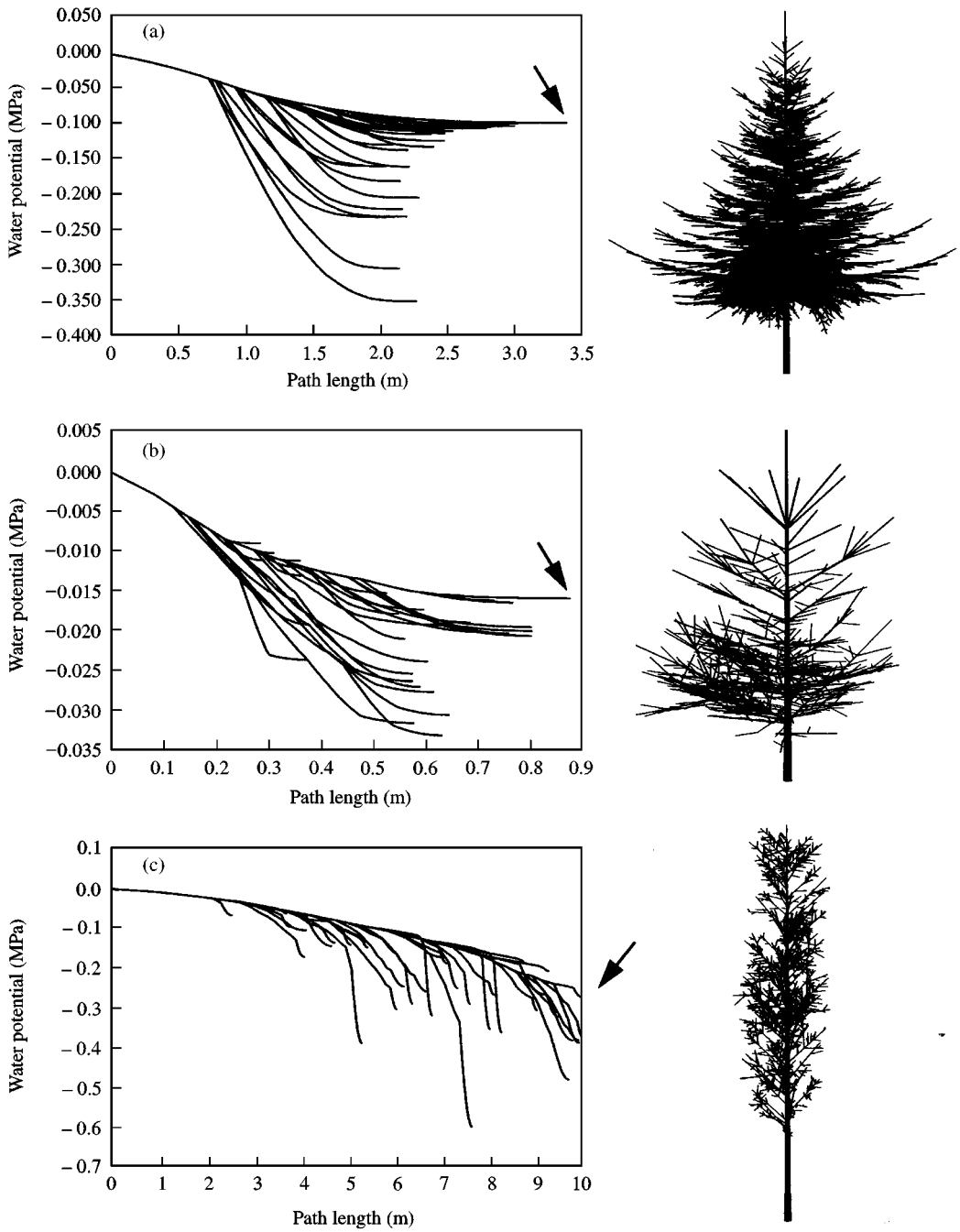

FIG. 3. Steady-state water potential profiles of (a) a 15-year-old *Picea abies* modeled by GROGRA, (b) a 12-year-old mapped *P. abies* and (c) a *Thuja occidentalis* mapped by Tyree (1988). From the flow paths of the trees, we selected the trunk and at least 20 first-order axes branching off at approximately equal distances. Path length of profile points is measured as distance from trunk base. Arrows point to the treetops.

(0.01 MPa m^{-1}). Comparing the gradients of trunk and branches at the junctions, we found that towards the treetop the branch gradients align with the low trunk gradients. Again, the mapped tree and the modeled tree exhibit the same pattern. In the model tree, the maximal branch gradient is about 0.25 MPa m^{-1} and exceeds the trunk gradient at the junction by a factor of about 4.2. In the mapped spruce, the corresponding values are 0.32 MPa m^{-1} and 7.6.

In contrast to *P. abies*, the gradients of *T. occidentalis* become steeper towards the ends of the axes. They only flatten out again close to the ends. The gradient of gravity is hardly exceeded at trunk base, while 0.04 MPa m^{-1} is reached at the treetop. The gradients of the branch bases are only slightly steeper, sometimes even lower than the gradients of the trunk, whereas the gradients of the branch tips reach up to 1.5 MPa m^{-1}.

A steady-state water potential profile is determined by the *LSC* pattern in the tree crown. The distribution of diameters [via the species-specific $\hat{K}(d)$ regressions], of leaf areas, and the numbers of daughter axes per length of the mother axis are influencing factors. Thus, the consistency between the profiles of the modeled and the mapped *P. abies* suggests that the growth grammar of Kurth and Früh (1999) reflects branching morphology correctly. Interpreting the differences between the profiles of *P. abies* and *T. occidentalis* leads to a connection with leaf distribution (data not shown). In the cylindrical crown of *T. occidentalis*, the leaves are concentrated in a peripheral crown mantle. The thickness of the mantle exhibits little variation with height. Water potential gradients of the branches peak within this mantle. Since the gradients of the branch bases are not markedly steeper than the trunk gradients, the hydraulic segmentation, *sensu* Zimmermann (1983), takes place *within* the peripheral crown mantle. In young spruces, a conical crown core with low leaf density extends from the base to the middle of the crown (Burger, 1939). The modeled spruce follows this pattern more clearly than the mapped spruce. The gradients of the branches are maximal within the crown core and minimal within the surrounding crown zone. Thus, the segmentation is between the leafy zone and the trunk. However, even in the lower crown parts, the segmentation is markedly less pronounced than in *T. occidentalis*. In *P. abies*, we would expect the following onset of cavitation dynamics: in the radial direction, the leafy crown zone would be caught quite uniformly by the impairment of water supply, the risk of impairment would increase from treetop to crown base, and the impairment might rapidly spread to the trunk. In *T. occidentalis*, the 5% level of conductivity loss is reached at a water potential about 0.5 MPa higher than in *P. abies* (Sperry & Tyree, 1990; Cochard, 1992). But because of the pronounced differentiation of potentials within the leafy crown mantle, we would predict a less fatal course of nonlinear dynamics. These hypotheses are consistent with the known differences in the drought tolerance of both species. The drought-avoiding *P. abies* closes its stomata during an early stage of drought, starting with the lowest third of the crown (Pisek & Tranquilini, 1951). *T. occidentalis* grows in low-competition habitats contrasting hydrologically from wet to extremely dry (Collier & Boyer, 1989). It maintains high rates of gas exchange also under drought (Musselman *et al.*, 1975).

LOW-PASS CHARACTERISTICS OF TREES AS A FUNCTION OF ARCHITECTURE

Kramer (1937) reported a lag between transpiration and root water uptake, which he explained by water storage in the shoot. Today, studies of hydraulic leaf-to-root signalling still use the term lag and explain it by a stored amount of water (e.g. Schulze *et al.*, 1985). However, spatially distributed systems, which are governed by a diffusion equation [eqn (6) and the discrete analogue eqn (11)], exhibit no lag between changes (signals) at one location and the response to these changes at another location. The input signal is not reproduced, but the system transmits the signal like a low-pass filter reducing the amplitude and introducing a phase shift. Both amplitude reduction and phase shift increase with the frequencies of the Fourier components (Schüssler, 1990). We expect from system theory that the low-pass characteristics of trees are determined by the spatial distribution of the capacities *and* conductivities within the hydraulic network structure (Oppenheim & Willsky, 1983; Schüssler, 1990). They do not result solely from the amount of water stored in the trunk and the leaves. The concepts of system theory may also account for more universality, at least in the case of linear water flow, which is realized far away from drought stress: the transmission behaviour of linear and time-invariant systems can be completely characterized by the response to a step signal (Oppenheim & Willsky, 1983).

What is the physiological relevance of the low-pass characteristics? In the diurnal cycles of root

water uptake, the periods of uptake are spread out and the peaks are reduced. As a consequence, the formation of perirhizal gradients, which strongly influence the water conduction in the soil and the water potential level of the tree, may be moderated. While a low shoot–root ratio distributes root water uptake spatially (Weatherley, 1970), the low-pass filtering by the shoot may act via a temporal distribution of water uptake.

A simulation study explored how the water flow at trunk base responds to step changes of transpiration flux density and how these transient flow responses vary with the tree architecture. As independent variable, we selected the sum of shoot lengths, which we regard as a measure reflecting structural complexity of the hydraulic network. A series of simulations was run with four mapped *P. abies* trees, with a succession of 6- to 21-year-old model trees generated by the *P. abies* growth grammar (Kurth & Früh, 1999) and with the *T. occidentalis* tree mapped by Tyree (1988). The simulation settings were the same as with the water potential profiles. The flow responses at trunk base were quantified by their half-times.

In all simulations, the flow at trunk base reacts like a low-pass filter. The temporal derivative of flow is maximal immediately after the application of the transpiration step. Thereupon the derivative gradually returns to zero until the new steady-state level of flow is reached (inset of Fig. 4). The half-times of mapped and modeled spruces increase with the sum of shoot lengths according to $y = 0.009x + 2.744$ ($R^2 = 0.958$). Since only young spruces with a small length sum were mapped, the regression is somewhat uncertain for these trees. However, the half-time of *T. occidentalis* is higher by a factor of 7.2 than the value resulting from the regression line.

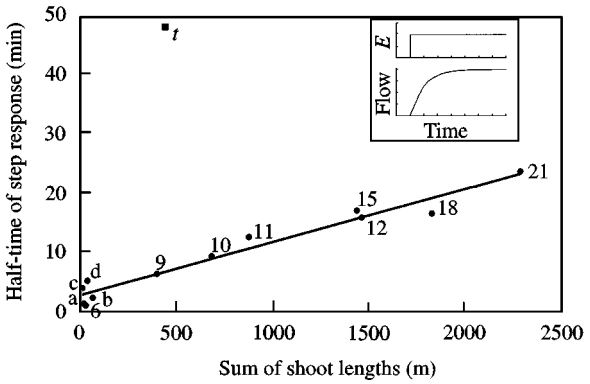

FIG. 4. Half-times of flow responses at trunk base vs. the sum of shoot lengths of several trees. Flow reacted like a low-pass filter to steps of transpiration flux density (inset). (a–d) represent mapped *P. abies* trees between 11 and 16-year-old. The points 6–21 are modeled *P. abies* trees of corresponding ages. The square labelled "*t*" is the *T. occidentalis* mapped by Tyree (1988).

The linear increase of half-times with length sum apparently depends on species. Further regressions (not shown) support the hypothesis that the low-pass characteristics are species-specific functions of a set of architectural quantities. The observed structure-function relationship reveals a perspective of simplification: from architectural quantities, it could be predicted how the transpiration signal of the crown is transmitted to the soil. This may be important for models of atmosphere-soil coupling, and it could improve the estimation of canopy conductance from sapflow data (Phillips *et al.*, 1997).

DROUGHT STRESS RESPONSES OF TREE VARIANTS WITH REDUCED CROSS-SECTIONS

Starting with a 15-year-old model tree generated by the *P. abies* growth grammar, architectural variants were produced by multiplying all axis cross-sections by a global reduction factor. Factors varied between 1.0 and 0.08. Trees were subjected to a scenario of drought stress: for 24 h the transpiration flux density remained at a level of $E = 1.0 \times 10^{-5}$ kg $s^{-1} m^{-2}$, the observed maximum of spruces; Ψ_{soil} was set to -1.0 MPa. At each location of a tree, leaf area was set to 0 when the local loss of conductivity exceeded 95%.

We found that in all tree variants, leaf mortality reaches steady state within 12 h. With reduction factors of cross-sections down to 0.4, no loss of leaf area occurs (Fig. 5). Steady-state leaf mortality does not go beyond the zero line until 0.3. Thereupon the 50% level is exceeded with high acceleration at 0.08. To check whether spatially extended impairments at a low level had been overlooked by the 95% rule, we studied profiles of conductivity loss. However, we found that with a reduction factor of 0.4, conductivity losses stay within 1% in all crown regions. With a factor of

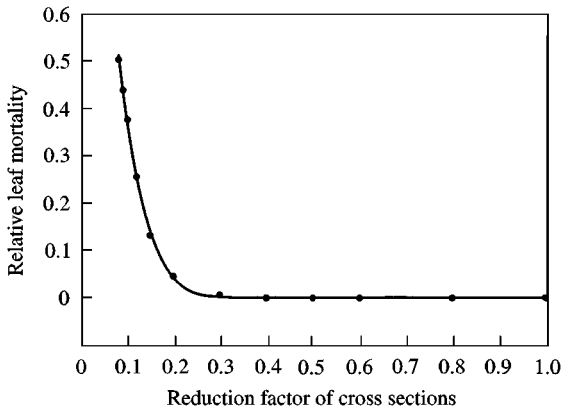

FIG. 5. Relative leaf mortality vs. reduction factor of cross-sections. The points represent variants of a 15-year-old modeled *P. abies* generated by reducing the cross-sections of all axes by a global factor. The trees were subjected to a high transpiration flux density ($E = 1.0 \times 10^{-5}$ kg s^{-1} m^{-2}) starting at $t = 0$ and to a $\Psi_{soil} = -1.0$ MPa. At each location of a tree, leaf area was set to 0 if the local conductivity loss exceeded 95%. Results are shown for $t = 12$ h, a time by which all tree variants have reached steady-state leaf mortality.

0.3, conductivity losses exceed 1% only in a few regions.

The results suggest that the dynamics caused by cavitation leads to a rapid breakdown of the hydraulic system when cross-sections fall below a critical limit. The dynamics seems to act like a threshold process comparable to the mechanical breakdown of tree structures (Mosbrugger, 1990). The results point to the necessity of a cybernetical control, which is tuned to the strong nonlinear dynamics in the hydraulic network. This may be an essential function of stomatal regulation. Jones & Sutherland (1991) predicted how stomatal conductance is constrained by cavitation. Our hypotheses are also consistent with observations that the stomata respond to hydraulic conductivity losses (Sperry & Pockman, 1993). However, reduction of gas exchange is costly (Cowan, 1982). Thus, we conclude from the observed critical limit of cross-sections that the dynamics under drought imposes sharp constraints on the construction of trees. The tolerance to reductions of cross-sections down to a factor of 0.3 appears as a safety margin. Safety margins in general accompany structural optimization of organisms (Mosbrugger, 1990).

Conclusions

The theoretical framework presented is an improvement over previous models which compute water flow in branched tree architectures. In these models, the consistency between the underlying physiological assumptions and the discrete computation method was not ensured. In contrast, our theoretical derivation and model tests corroborate the consistent translation of the underlying assumptions. The numerical simulation model HYDRA has not yet been empirically tested. However, we have fulfilled an elementary precondition: a comparison between model results and empirical data allows conclusions about the validity of the underlying assumptions. We feel that tree water flow modelling has now met with the standards of simulation established in hydrology (see *Introduction*).

We further contribute towards a better understanding of hydraulic integration and also to more universality by uniting different phenomena of the hydraulic system of trees. To the authors' knowledge, it is for the first time that Darcy flow, water storage and conductivity losses in the hydraulic network are represented by one discrete IBVP. It is one model which is able to compute nonlinear, non-steady-state flow under drought stress as well as the limit case of linear, steady-state flow.

Our theoretical description makes no claim to be exhaustive. It is a framework also in the sense that aspects currently missing (leaf-shoot resistance, spatial variability of transpiration flux density, stomatal control) can be supplemented without touching it in its substance. However, we see natural bounds to extending the theory. In the preliminaries, we gave reasons for the restriction to the above-ground tree parts. It does not appear possible to reflect water flow dynamics in the soil–plant–atmosphere continuum via one uniform theory. It is rather necessary to couple different modelling approaches, ones that are separately valid for soil–root space, above-ground tree parts and the crown atmosphere. To take into account the atmospherical driving forces of transpiration, we attempted to couple HYDRA with a three-dimensional model of microclimatics (Lanwert *et al.*, 1998). We intend to connect the above-ground tree parts with the

soil–root space by linking HYDRA to the soil water flow model silVlow (Blendinger, 1995), which includes the distribution of fine roots and the root water uptake.

Beyond these contributions, the numerical simulation model HYDRA is an efficient tool for structure–function studies. The following features enable us to treat tree architecture as independent variable: (1) linkage to the tree growth model GROGRA, which can generate and process tree maps (Kurth & Früh, 1999), (2) standardized discretization of tree architectures, (3) simple adjustment of functional information when tree architecture is exchanged, and (4) only linear increase of the computational demand per time step with the number of tree segments.

Simulation studies demonstrated our possibilities of deriving theoretically well-founded hypotheses about the behaviour of the hydraulic system. The model proved to be a powerful calculation tool which integrates data from empirical decompositions of the system. The studies also showed the usefulness of computer experiments. Input signals can be easily defined and reproduced to quantify system dynamics from the signal response. These possibilities enabled us to formulate new hypotheses on the following points: (1) differences in the hydraulic segmentation between *P. abies* and *T. occidentalis*, (2) responses to rapid transpiration changes and to a scenario of drought stress, and (3) how these responses depend on architectural quantities of the trees.

We have presented a contribution to the theory of the hydraulic system of trees. The structure–function relationships of trees and the problem of hydraulic integration have far-reaching ecological implications. As already discussed, trees are integral parts of the soil–plant–atmosphere continuum. There is also the fact that the water and carbon relations of plants are closely interwoven (Küppers, 1984; Tyree & Alexander, 1993). We see our work in the context of recent approaches in ecological modelling which endeavour to link physiological processes to the structures of trees and tree stands (Hauhs *et al*., 1995; De Reffye *et al*., 1997).

This work was a part of the Forschungszentrum Waldökosysteme Göttingen supported by the German Bundesministerium für Bildung, Wissenschaft, Forschung und Technologie. We greatly appreciate the involvement of B. Sloboda in promoting the plant-modelling group in Göttingen. S. Schmidt, J. Schmidt, R. Schaback, G. Lischeid and D. Lanwert gave constructive criticism and other valuable inputs. We thank G. Anzola for the mapping of young spruces. We further acknowledge the kind permission of M. T. Tyree to publish the results based on the data of the *Thuja occidentalis* tree.

REFERENCES

ABBOTT, M. B. & REFSGAARD, J. C. (eds) (1996). *Distributed Hydrological Modelling*. Dordrecht: Kluwer Academic Publishers.

AMES, W. F. (1977). *Numerical Methods for Partial Differential Equations*. New York: Academic Press.

BLENDINGER, C. (1995) silVlow—ein Programm zur Berechnung gesättigt-ungesättigter Strömung im zweidimensionalen porösen Medium. *Schriftenreihe* SFB 350, Universität Bonn.

BORGHETTI, M., EDWARDS, W. R. N., GRACE, J., JARVIS, P. G. & RASCHI, A. (1991). The refilling of embolized xylem in *Pinus sylvestris* L. *Plant Cell Environ.* **14,** 357–369.

BRAUN, H. J. (1970). Funktionelle Histologie der sekundären Sproßachse. I. Das Holz. *Handbuch der Pflanzenanatomie*, Vol. IX, pp. 1–190. Berlin und Stuttgart. Gebrüder Borntraeger.

BURGER, H. (1939). Der Kronenaufbau gleichalteriger Nadelholzbestände. *Mitteil. Schweiz. Anst. forstl. Versuchswesen* **21,** 5–57.

ČERMÁK, J., DEML, M. & PENKA, M. (1976). Improvement of the method of sap flow rate determination in full-grown trees based on heat balance with direct electric heating of xylem. *Biol Plantar.* **18,** 105–110.

COCHARD, H. (1992). Vulnerability of several conifers to air embolism. *Tree Physiol.* **11,** 73–83.

COLLIER, D. E. & BOYER, M. G. (1989). The water relations of *Thuja occidentalis* L. from two sites of contrasting moisture availability. *Bot. Gaz.* **150,** 445–448.

COWAN, I. R. (1982). Regulation of water use in relation to carbon gain in higher plants. In: *Encyclopedia of Plant Physiology* 12 *B*: *Water Relations and Carbon Assimilation*. (Pirson, A. & Zimmermann, M. H., eds), Berlin: Springer.

DE REFFYE, P., FOURCAUD, T., BLAISE, F., BARTHÉLÉMY, D. & HOULLIER, F. (1997). A functional model of tree growth and tree architecture. *Silva Fennica* **31,** 297–311.

DOUGLAS, J. JR. (1961). A survey of numerical methods for parabolic differential equations. *Adv. Computer* **2,** 1–54.

DOUGLAS, J. JR. & HORNUNG, U. (eds) (1993). Flow in porous media. *Proc. Oberwolfach Conference*, 21–27 June, 1992. International Series of Numerical Mathematics, Vol. 114. Basel: Birkhäuser.

DOUGLAS, J. & JONES, B. F. (1963). On predictor–corrector methods for nonlinear parabolic differential equations. *J. Soc. Indust. Appl. Math.* **11,** 195–204.

DOUSSAN, C., PAGÈS, L. & VERCAMBRE, G. (1998). Modelling of the hydraulic architecture of root systems: an integrated approach to water absorption—model description. *Ann. Bot.* **81,** 213–223.

EDWARDS, W. R. N. & JARVIS, P. R. (1982). Relation between water content, potential and permeability in stems of conifers. *Plant Cell Environ.* **5,** 271–277.

EDWARDS, W. R. N., JARVIS P. G., LANDSBERG, J. J. & TALBOT, H. (1986). A dynamic model for studying flow of water in single trees. *Tree Physiol.* **1,** 309–324.

EWERS, F. & ZIMMERMANN, M. H. (1984). The hydraulic architecture of balsam fir (*Abies balsamea*). *Physiol. Plant* **60,** 453–458.

FEDDES, R. A., KABAT, P., VAN BAKEL, P. J. T., BRONSWIJK, J. J. B. & HALBERTSMA, J. (1988). Modelling soil water dynamics in the unsaturated zone—state of the art. *J. Hydrol.* **100,** 69–112.

FRÜH, TH. (1995). Entwicklung eines Simulationsmodells zur Untersuchung des Wasserflusses in der verzweigten Baumarchitektur. *Ber Forschungszentr Waldökosysteme Göttingen* **A 131**.

GARDNER, G. (1960). Dynamic aspects of water availability of plants. *Soil Sci.* **89,** 63–73.

GRANIER, A. (1987). Mesure du flux de sève brute dans le tronc du Douglas fir par une nouvelle méthode thermique. *Ann. Sci. For.* **44,** 1–14.

GROSSMANN, C. & ROOS, H. G. (1992). *Numerik partieller Differentialgleichungen*. Stuttgart: Teubner.

HATHEWAY, W. H. & WINTER, D. F. (1981). Water transport and storage in Douglas–fir: a mathematical model. *Mitteil Forstl BVA Wien* **142,** 193–222.

HAUHS, M., KASTNER-MARESCH, A. & ROST-SIEBERT, K. (1995). A model relating forest growth to ecosystem–scale budgets of energy and nutrients. *Ecol. Modell.* **83,** 229–243.

HORNUNG, U. & MESSING, W. (1984). *Poröse Medien und Simulation*. Kirchzarten: Verlag Beiträge zur Hydrologie.

ISTOK, J. D. (1989). *Groundwater Modeling by the Finite Element Method*, Water Resources Monograph 13. Washington, DC: American Geophysical Union.

JARVIS, P. G. (1975). Water transfer in plants. In: *Heat and Mass Transfer in the Biosphere*. (De Vries, D. A. & Afgan, N. H., eds), New York: John Wiley & Sons.

JONES, H. G. & SUTHERLAND, R. A. (1991). Stomatal control of xylem embolism. *Plant Cell Environ.* **14,** 607–612.

KATZ, C., OREN, R., SCHULZE, E.-D. & MILBURN, J. A. (1989). Uptake of water and solutes through twigs of *Picea abies* (L.) Karst. *Trees* **3,** 33–37.

KRAMER, P. J. (1937). The relation between rate of transpiration and rate of absorption of water in plants. *Am. J. Bot.* **24,** 10–15.

KUČERA, J., ČERMÁK, J. & PENKA, M. (1977). Improved thermal method of continual recording the transpiration flow rate dynamics. *Biol. Plantar* **19,** 413–420.

KÜPPERS, M. (1984). Carbon relations and competition between woody species in a central European hedgerow. Part II: stomatal responses, water use, and hydraulic conductivity in the root/leaf pathway. *Oecologia* **64,** 344–354.

KURTH, W. (1994). Growth Grammar Interpreter GROGRA 2.4. A software tool for the 3-dimensional interpretation of stochastic, sensitive growth grammars in the context of plant modelling. *Ber Forschungszentr Waldökosysteme* **B 38**.

KURTH, W. & FRÜH, TH. (1999). Modelling crown structure of conifers: a stochastic growth grammar for the developing branching system of spruce (submitted).

LAFOLIE, F., BRUCKLER, L. & TARDIEU, F. (1991). Modeling root water potential and soil–root water transport: I. Model presentation. *Soil Sci. Soc. Am. J.* **55,** 1203–1212.

LANDSBERG, J. J., BLANCHARD, T. W. & WARRIT, B. (1976). Studies on the movement of water through apple trees. *J. Exp. Bot.* **27,** 579–596.

LANWERT, D., DAUZAT J. & FRÜH, TH. (1998). Water use of forest trees: a possibility of combining structural and functional models. *Bayreuther Forum Ökologie* **52,** 117–128.

LAPIDUS, L. & PINDER, G. F. (1982). *Numerical Solution of Partial Differential Equations in Science and Engineering*. New York: Wiley.

MANTEUFFEL, T. A. & WHITE A. B. JR. (1986). The numerical solution of second-order boundary value problems on nonuniform meshes. *Math. Comp.* **47,** 511–535.

MILBURN, J. A. (1979). *Water Flow in Plants*. London: Longman.

MOHR, H. & SCHOPFER, P. (1993). *Pflanzenphysiologie*. Berlin: Springer.

MOSBRUGGER, V. (1990). *The Tree Habit in Land Plants*, Lecture Notes in Earth Sci., vol. 28. Berlin: Springer.

MUNZ, P. (1985). *Our Knowledge of the Growth of Knowledge–Popper or Wittgenstein*? London: Routledge & Kegan Paul.

MUSSELMAN, R. C., LESTER, D. T. & ADAMS, M. S. (1975). Localized ecotypes of *Thuja occidentalis* L. in Wisconsin. *Ecology* **56,** 647–655.

OPPENHEIM, A. V. & WILLSKY, A. S. (1983). *Signals and Systems*. Englewood Cliffs, NJ: Prentice-Hall.

PETTY, J. A. & PALIN, M. A. (1983). Permeability to water of the fibre cell wall material of two hardwoods. *J. Exp. Bot.* **34,** 688–693.

PHILLIPS, N., NAGCHAUDHURI, A., OREN, R. & KATUL, G. (1997). Time constant for water transport in loblolly pine trees estimated from time series of evaporative demand and stem sapflow. *Trees* **11,** 412–419.

PISEK, A. & TRANQUILINI, W. (1951). Transpiration und Wasserhaushalt der Fichte (*Picea excelsa*) bei zunehmender Luft- und Bodentrockenheit. *Physiol. Plant.* **4,** 1–27.

POCKMAN, W. T., SPERRY, J. S. & O'LEARY, J. W. (1995). Sustained and significant negative water pressure in xylem. *Nature* **378,** 715–716.

PRESS, W. H., TEUKOLSKY, S. A., VETTERLING, W. T. & FLANNERY, B. P. (1992). *Numerical Recipes in C. The Art of Scientific Computing*. Cambridge: Cambridge University Press.

RITCHIE, G. A. & HINCKLEY, T. M. (1975). The pressure chamber as an instrument for ecological research. *Adv. Ecol. Res.* **9,** 165–254.

RUNNING, S. W., WARING, R. H. & RYDELL, R. A. (1975). Physiological control of water flux in conifers. A computer simulation model. *Oecologia* **18,** 1–16.

SCHULZE, E. D., ČERMÁK, J., MATYSSEK, R., PENKA, M., ZIMMERMANN, R., VASIČEK, F., GRIES, W. & KUČERA, J. (1985). Canopy transpiration and water fluxes in the xylem of the trunk of *Larix* and *Picea* trees—a comparison of xylem flow, porometer and cuvette measurements. *Oecologia* **66,** 475–483.

SCHÜSSLER, H. W. (1990). *Netzwerke, Signale und Systeme. Band 2: Theorie kontinuierlicher und diskreter Signale und Systeme*. Berlin: Springer.

SELLIN, A. (1991). Hydraulic conductivity of xylem depending on water saturation level in Norway spruce (*Picea abies* [L.] Karst.). *J. Plant Physiol.* **138,** 466–469.

SIAU, J. F. (1984). *Transport Processes in Wood*. Berlin: Springer.

SLATYER, R. O. (1967). *Plant–Water Relationships*. London: Academic Press.

SPERRY, J. S., DONNELLY, J. R. & TYREE, M. T. (1988). A method for measuring hydraulic conductivity and embolism in xylem. *Plant Cell Environ.* **11,** 35–40.

SPERRY, J. S., HOLBROOK, N. M., ZIMMERMANN, M. H. & TYREE, M. T. (1987). Spring filling of xylem vessels in wild grapevine. *Plant Physiol.* **83,** 414–417.

SPERRY, J. S. & IKEDA, T. (1997). Xylem cavitation in roots and stems of Douglas-fir and white fir. *Tree Physiol.* **17,** 275–280.

SPERRY, J. S. & POCKMAN, W. T. (1993). Limitation of transpiration by hydraulic conductance and xylem cavitation in *Betula occidentalis*. *Plant Cell Environ.* **16,** 279–287.

SPERRY, J. S. & TYREE, M. T. (1990). Water-stress-induced xylem embolism in three species of conifers. *Plant Cell Environ.* **13,** 427–436.

SWAMY, M. N. S. & THULASIRAMAN, K. (1981). *Graphs, Networks and Algorithms*. New York: John Wiley & Sons.

TROMPERT, R. A. & VERWER, J. G. (1990). Runge–Kutta-methods and local uniform grid refinement. Report NM-R9022, Centre for Mathematics and Computer Science, Amsterdam.

TYREE, M. T. (1988). A dynamic model for water flow in a single tree: evidence that models must account for hydraulic architecture. *Tree Physiol.* **4,** 195–217.

TYREE, M. T. & ALEXANDER, J. D. (1993). Plant water relations and the effects of elevated CO_2: a review and suggestions for future research. *Vegetatio* **104/105,** 47–62.

TYREE, M. T. & COCHARD, H. (1996). Summer and winter embolism in oak: impact on water relations. In: *Ecology and Physiology of Oaks in a Changing Environment*. Selected papers from an *International Symposium*, September 1994, Nancy, France. (Dreyer, E., ed.), *Ann. Sci. For.*, **53,** pp. 173–180.

TYREE, M. T. & EWERS, F. (1991). Tansley Review No. 34: The hydraulic architecture of trees and other woody plants. *New Phytol.* **119,** 345–360.

TYREE, M. T., GRAHAM, M. E. D., COOPER, K. E. & BAZOS, L. J. (1983). The hydraulic architecture of *Thuja occidentalis*. *Can. J. Bot.* **61,** 2105–2111.

TYREE, M. T. & SPERRY, J. S. (1988). Do woody plants operate near the point of catastrophic xylem dysfunction caused by dynamic water stress? Answers from a model. *Plant Physiol.* **88,** 574–580.

TYREE, M. T. & SPERRY, J. S. (1989). Vulnerability of xylem to cavitation and embolism. *Ann. Rev. Plant. Phys. Mol. Biol.* **40,** 19–38.

TYREE, M. T. & YANG, S. (1990). Water-storage capacity of *Thuja*, *Tsuga* and *Acer* stems measured by dehydration isotherms. *Planta* **182,** 420–426.

VON ROSENBERG, D. U. (1969). *Methods for the Numerical Solution of Partial Differential Equations*. New York: American Elsevier.

WARING, R. H., WHITEHEAD, D. & JARVIS, P. G. (1979). The contribution of stored water to transpiration in Scots pine. *Plant Cell Environ* **2,** 309–317.

WATKINS, D. S. (1991). *Fundamentals of Matrix Computations*. Chichester, Wiley.

WEATHERLEY, P. E. (1970). Some aspects of water relations. *Adv. Bot. Res.* **3,** 171–206.

WILSON, K. & WHITE, D. J. B. (1986). *The Anatomy of Wood: its Diversity and Variability*. London: Stobart & Son Ltd.

YANG, S. & TYREE, M. T. (1994). Hydraulic architecture of *Acer saccarum* and *A. rubrum*: comparison of branches to whole trees and the contribution of leaves to hydraulic resistance. *J. Exp. Bot.* **45,** 179–186.

ZIMMERMANN, M. H. (1978). Hydraulic architecture of some diffuse-porous trees. *Can J. Bot.* **56,** 2286–2295.

ZIMMERMANN, M. H. (1983). *Xylem Structure and the Ascent of Sap*. Berlin: Springer.